Hindawi

Research Article

Experimental Study on Dynamic Performance of Rock-Concrete Composite with Different Thickness Ratios

Qi Ping [1,2,3] **Kaifan Shen,** [2,3] **Qi Gao,** [2,3] **Chen Wang,** [2,3] **Shuo Wang,** [2,3] **Yulin Wu,** [2,3] **and Jing Hu** [2,3]

[1]*State Key Laboratory of Mining Response and Disaster Prevention and Control in Deep Coal Mine,
Anhui University of Science and Technology, Huainan, Anhui 232001, China*
[2]*Research Center of Mine Underground Engineering, Ministry of Education, Anhui University of Science and Technology,
Huainan, Anhui 232001, China*
[3]*School of Civil Engineering and Architecture, Anhui University of Science and Technology, Huainan, Anhui 232001, China*

Correspondence should be addressed to Qi Ping; ahpingqi@163.com

In order to study the influence of different thickness ratios on the mechanical properties of rock-concrete composite, a 50 mm diameter split Hopkinson pressure bar device (SHPB) was used to conduct impact loading tests on ϕ 50 mm × 50 mm cylindrical composite with sandstone thickness of 0, 5, 10, 15, 20, 25, 30, 35, 40, 45, and 50 mm. The results show that with the increase of the proportion of rock in the composite, the dynamic compressive strength increases gradually, and the dynamic elastic modulus increases linearly. When the rock thickness increases, the average strain rate decreases and the peak strain decreases. In dynamic loading combination behind the rock specimen with concrete cushion, absorb energy decrease with the increase of rock accounted concrete; when the rock is 25 mm, total absorption energy reached its lowest point; when the thickness of the rock is greater than the thickness of concrete, concrete and adjacent parts of rock joint cushion absorb the energy into a rising trend. With the increase of the proportion of rock, the degree of fragmentation of the composite specimens decreases gradually, and the fragments are mostly concrete with smaller particle size, which is correlated with the dynamic compressive strength. The rock-concrete interface is a weak surface relative to the materials on both sides.

1. Introduction

Rock-concrete interface structures are common in many engineering practices, such as large hydropower stations, road tunnels, and mine construction. In the process of cross-operation, such projects often adopt the method of blasting excavation and mechanical excavation in stages, which not only improves the construction efficiency but also exerts great force on the surrounding rock strata. The vibration wave generated by the construction excavation in the subsequent stages is transmitted to the completed part. Seismic waves can also affect structures. Qu et al. [1–5] conducted relevant research on seismic Earth pressure and support design. The influence of rock-concrete structure is different with the thickness of rock strata.

Many scholars have carried out a series of experimental studies on composite rock mass and achieved fruitful results. In static compression test research, Zuo et al. [6] conducted uniaxial compression tests on coal-rock assemblage with different combinations and found that coal had a great influence on the strength of the assemblage. Liu et al. [7] conducted uniaxial compression tests on composite specimens with different material strengths, and the results showed that the overall strength of composite specimens was more significantly affected by the volume proportion of materials with higher strength. Zhao et al. [8] carried out uniaxial compression tests on specimens of composite with different coal thicknesses, and the results showed that with the increase of coal thickness, the compressive strength of specimens gradually decreased, and the composite changed

from tensile failure to shear failure. Zhang et al. [9] conducted compression tests on coal and rock mass in different combinations and found that the damage was mainly concentrated in the coal part, and the damage and failure of the coal part would induce the damage and failure of rock mass. Gong et al. [10] conducted uniaxial compression tests on coal-rock assemblage with different low loading rates, and the results showed that with the increase of loading rates, the failure of the assemblage was transformed from coal to coal-rock assemblage. Zeng et al. [11] conducted uniaxial compression tests on specimens with different combinations of three types, and the results showed that composite specimens were greatly affected by medium with lower strength. Teng et al. [12] conducted uniaxial compression tests on six composite rock masses with different combination modes, and the results showed that the stress state of the composite body was determined by the combination mode. Zhu et al. [13] conducted cyclic loading and unloading tests on coal-rock assemblage and found that the internal structure and material properties of the specimen would affect loading and unloading. Yang et al. [14] believed that the strength of sandstone at the interface of coal-rock combination was "weakened" after true triaxial loading test on the coal-rock combination. Dong [15] carried out true triaxial static load test on the combination of different coal-rock ratios and found that the strength and elastic modulus of the combination were negatively correlated with the coal content.

In dynamic compression test research, Chen et al. [16] conducted dynamic compression tests on the concrete-frozen soil combination, and the study showed that the frozen soil behind the concrete absorbed part of the energy and played a buffer role during impact, when the strain rate was the same, the greater the absorption energy of the combination, the greater the damage degree of frozen soil sample, and the smaller the damage degree of concrete sample. Wen et al. [17] used 50 mm diameter Hopkinson bar to conduct dynamic compression tests on composite rock samples with different dip angles under different strain rates, and the results showed that the greater the absorption energy of the sample, the higher the dynamic crushing degree. Yang et al. [18] conducted separate Hopkinson pressure bar test on rocks with different joint thicknesses, and the dynamic compressive strength of jointed rocks gradually decreased with the increase of filling thickness. Yang et al. [19, 20] conducted dynamic compression tests on jointed rock specimens and composite rock mass, and found the influence of constituent materials on the mechanical properties of composite specimens. Guo et al. [21–23] conducted the SHPB dynamic test on early-age shotcrete-surrounding rock composite specimen, and the results showed that the dynamic characteristics of the composite specimen were greatly affected by early-age concrete. Chen et al. [24, 25] conducted dynamic and static compression tests on rock-steel fiber concrete composite layer specimens. After comparative analysis, they believed that the content of steel fiber had a great influence on the compressive strength of the composite layer, and the compressive strength of the composite specimen was more significantly affected by the

strength of the concrete matrix. Miao et al. [26] conducted dynamic compression tests on rock-coal-rock combination specimens under different strain rates, and the breakage degree of specimens increased with the increase of strain rates.

To sum up, the current research on the specimens of combination of different materials has been relatively complete, but the previous research mainly focused on the mechanical experiment of the same thickness of constituent materials, and the research on the combination of different material proportions still needs to be supplemented and improved. In this paper, SHPB impact loading tests are carried out on concrete-rock assemblage specimens with a volume of ϕ 50 mm × 50 mm and sandstone thickness of 0~50 mm with a gradient of 5 mm.

2. Experimental Study

2.1. Assembly Specimen Processing and Preparation. In the test, the concrete used in the actual project quality mix ratio is cement : sand : stone : water = 1 : 1.5 : 3 : 0.58, cement is 42.5 grade ordinary Portland cement, sand used is coarse sand, and the gravel particle size is 5~15 mm. The rock is selected from the sandstone of Dingji Coal Mine in Huainan, Anhui Province. When preparing the composite specimen, the sandstone specimen with polished end face is vertically inserted into concrete. In order to be closer to the actual engineering situation, the natural conservation of concrete is also carried out in this test. After 28 days of natural curing, core, cutting, and grinding were carried out according to ISRM test standard [27] so that the nonparallelism of the two end faces of the specimen was less than or equal to 0.3 mm, and the axial deviation of the specimen perpendicular to the end face was less than or equal to 0.25°. A cylindrical composite specimen with ϕ 50 mm × 50 mm sandstone thickness of 0, 5, 10, 15, 20, 25, 30, 35, 40, 45, and 50 mm is processed, as shown in Figure 1.

2.2. Test Equipment. The SHPB loading system of State Key Laboratory of Mining Response and Disaster Prevention and Control in Deep Coal Mine was used in the test equipment, as shown in Figure 2.

The basic configuration of the instrument includes the impact loading system, axial loading system, gas sealing system, and data acquisition system. The incident bar, transmission bar, and absorption bar are made of the same alloy steel material, with a diameter of 50 mm, elastic modulus of 210 GPa, and yield strength greater than 800 MPa.

The special-shaped punch (SHPB international test standard for dynamic mechanics) was used in the test. It was loaded with half sine wave [28], and the material was the same as the incident bar.

2.3. Test Plan. In this experiment, rock-concrete combination is taken as the main research object. For the height of 50 mm, diameter of 50 mm, sandstone thickness of 0, 5, 10, 15, 20, 25, 30, 35, 40, 45, and 50 mm, that is, the ratios of rock
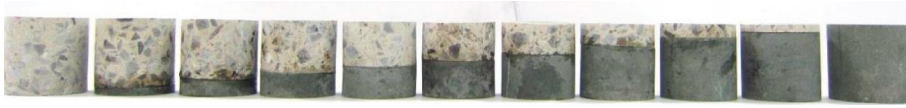
Figure 1: Processing prepared combined bodies.

Figure 2: SHPB test apparatus.

thickness to concrete thickness are 0:10, 1:9, 2:8, 3:7, 4:6, 5:5, 6:4, 7:3, 8:2, 9:1, and 10:0; a total of 11 groups of cylinder specimens were subjected to SHPB impact loading test. Each group of parallel tests has more than three specimens. After many tests, the 0.3 MPa pneumatic impact specimen was used. The clamping state of the specimen is shown in Figure 3. The rock surface is attached to the end of the incident bar. The mechanical properties and change rules of rock-concrete composite specimens with different thickness ratios are studied.

3. Analysis of Test Data

Table 1 shows typical results of SHPB impact compression test of rock-concrete composite specimens with different thickness ratios. In Table 1, σ is the dynamic compressive strength of specimens; ε is peak strain of specimen; $\dot{\varepsilon}$ frame is the average strain rate of specimens; E_d is the dynamic elastic modulus of specimen.

3.1. Stress-Strain Relationship Analysis. The three-wave method was used to process the collected data, and the dynamic compression stress-strain curve was obtained, as shown in Figure 4.

As can be seen from Figure 4, with the increase of rock-concrete thickness ratio, the composite body gradually changes from concrete to rock, and the dynamic compressive strength keeps increasing. The slope of the curve increases.

3.2. Analysis of Relation between Thickness Ratio and Dynamic Compressive Strength of Composite Body. In order to study the relationship between the dynamic compressive strength of specimens and the thickness ratio of composite materials, a scatter plot was drawn with the thickness of part of rock in the composite as the abscissa and the dynamic compressive strength as the ordinate, and linear fitting was adopted to

obtain the straight line as shown in Figure 5. The fitting effect was good, and the fitting relationship was as follows:

$$\sigma = 0.536L + 29.496 \left(R^2 = 0.9958 \right). \tag{1}$$

It can be seen from Figure 5 that the dynamic compressive strength of the composite specimen increases linearly with the increase of rock thickness and is positively correlated. This is because the rock strength is greater than the concrete strength. The overall strength of specimen increases with the increase of rock proportion.

Figure 6 shows the relationship between dynamic compressive strength and average strain rate of rock-concrete composite specimens with different thickness ratios, and the fitting equation is as follows:

$$\sigma = -0.020\dot{\varepsilon}^2 + 0.881\dot{\varepsilon} + 62.240 \left(R^2 = 0.9743 \right). \tag{2}$$

It can be seen from Table 1 that the average strain rate decreases with the increase of rock thickness in the composite. It can be seen from Figure 6 in this paper that, the dynamic compressive strength of the composite specimen in this paper increases with the decrease of strain rate. Because concrete is more fragile than rock, it is easier to produce deformation under the action of stress, and it is the main deformation bearer in the combination. With the decrease of the proportion of concrete and the increase of the proportion of rock, the average strain rate of specimens decreases and the dynamic compressive strength increases.

3.3. Analysis of Relation between Thickness Ratio and Dynamic Elastic Modulus of Composite Body. Figure 7 shows the relation curve between rock thickness and dynamic elastic modulus of composite specimens with different thickness ratios under the same loading pressure. It can be seen from the diagram that with increasing thickness of rock, the specimen shows linear elastic modulus scale growth trend and the dynamic compressive strength with the rock thickness change rule. This is because the combination of the
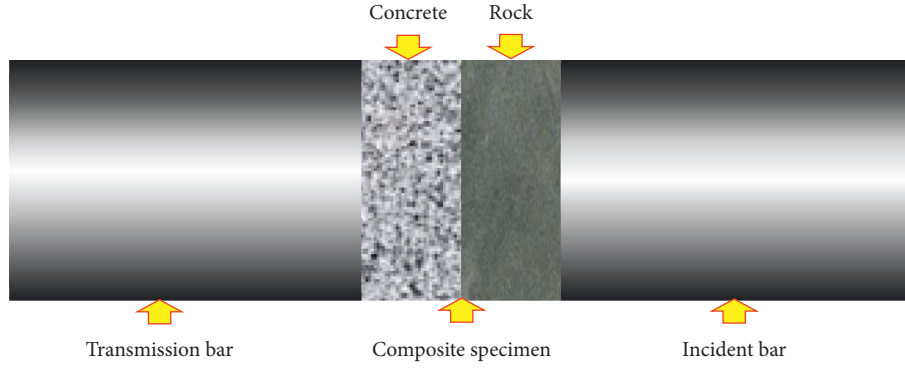
FIGURE 3: The clamping state of the specimen.

TABLE 1: SHPB shock compression test results of concrete-rock combined bodies with different thickness ratios.

| Specimen number	Specimen thickness (mm)		Thickness ratio	σ (MPa)	ε (10^{-3})	$\dot{\varepsilon}$ (s^{-1})	E_d (GPa)
	Rock	Concrete					
C-2	0	50	0:10	28.98	6.88	71.7	5.63
DJ21-03	5	45	1:9	32.91	6.32	70.5	13.17
DJ21-09	10	40	2:8	35.38	5.82	68.5	23.01
DJ21-13	15	35	3:7	37.11	5.33	66.1	26.03
DJ21-21	20	30	4:6	40.00	5.23	65.6	37.06
DJ21-27	25	25	5:5	43.14	4.77	64.1	43.98
DJ21-32	30	20	6:4	44.71	4.28	60.1	52.90
DJ21-37	35	15	7:3	48.47	4.31	58.4	57.61
DJ21-43	40	10	8:2	50.45	4.16	56.2	67.9
DJ21-49	45	5	9:1	53.62	3.75	53.1	79.27
DJ21-57	50	0	10:0	56.88	2.99	46.1	86.52
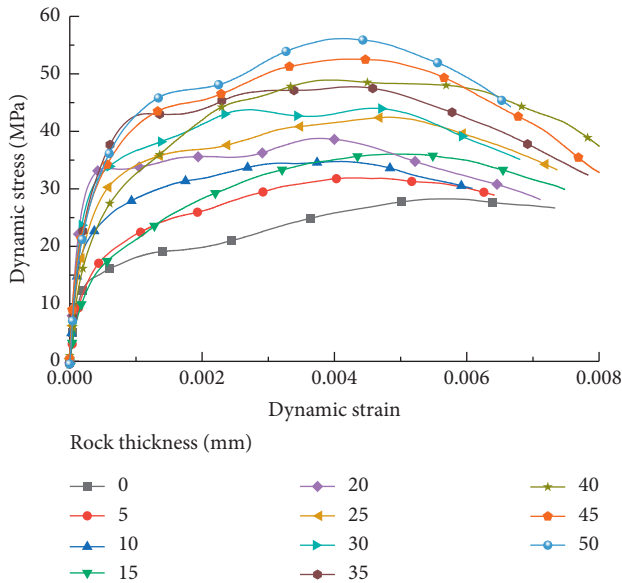
FIGURE 4: Dynamic stress-strain curves of rock-concrete combined bodies.

hard rock part is concrete, is not easy to produce strain, and is the main strength of combination specimens, considering rock proportion increase and elastic modulus increase. After fitting, the following linear relation is obtained:

$$E_d = 1.605L + 4.711 \left(R^2 = 0.9947 \right). \tag{3}$$

3.4. Analysis of Relation between Thickness Ratio and Peak Strain of Composite.

Under the same loading conditions, the peak strain of the rock-concrete composite specimen decreases with the increase of rock thickness, and the downward trend is relatively stable, as shown in Figure 8. The quadratic polynomial obtained by fitting is as follows:

$$\varepsilon = 3.431 \times 10^{-4} L^2 - 0.086L + 6.737 \left(R^2 = 0.9663 \right). \tag{4}$$

3.5. Analysis of Energy Dissipation of Composite Specimen.

Table 2 shows the energy dissipation test data of rock-concrete composite specimens with different thickness ratios. The incident energy is basically unchanged under the same impact pressure.

With the increase of rock thickness, the reflected energy decreases in a quadratic function trend, the absorbed energy decreases first and then increases at the turning point of rock thickness: concrete thickness = 1:1, and the transmitted energy increases in a nearly linear relationship. This is because the rock surface is attached to the end of the incident bar, so there are fewer cracks in the rock, the density is higher than that of concrete, and the wave impedance is higher. The transmission coefficient increases with the
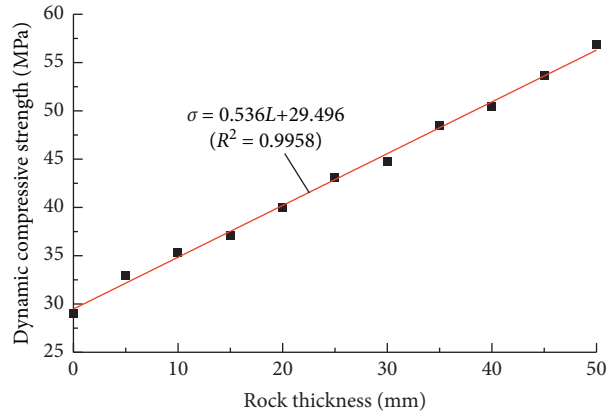
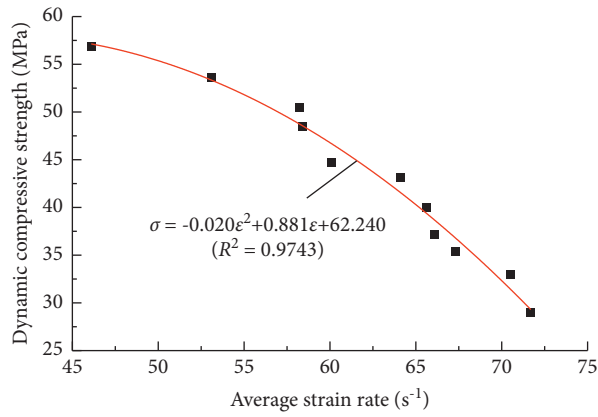FIGURE 5: Fitting line of rock thickness and dynamic compressive strength change.

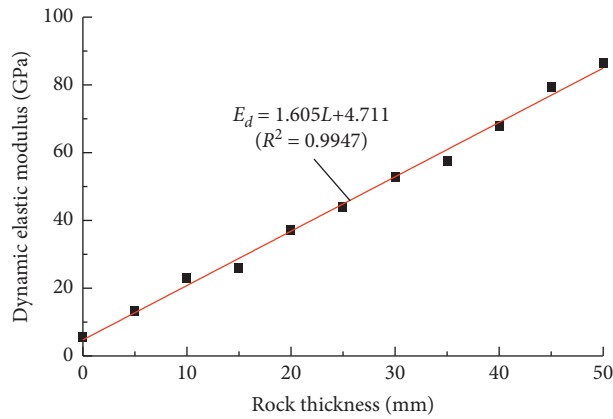FIGURE 6: Fitting curve of dynamic compressive strength and average strain rate.

FIGURE 7: Fitting line of relationship between rock thickness and dynamic elastic modulus.
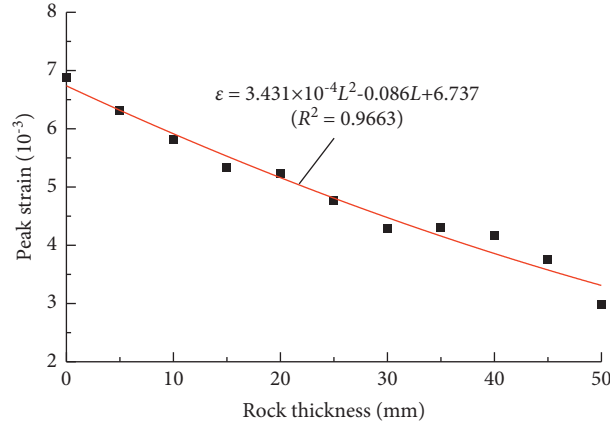
FIGURE 8: Fitting curve of relationship between rock thickness and peak strain.

TABLE 2: Energy data of rock-concrete composite specimens with different thickness ratios.

Specimen number	Energy (J)			
	Incident	Reflected	Transmitted	Absorbed
C-2	62.94	38.54	3.17	21.32
DJ21-03	62.15	38.35	4.14	19.66
DJ21-09	61.97	37.81	5.22	18.95
DJ21-13	60.95	37.75	5.05	18.15
DJ21-21	61.24	37.88	6.34	17.02
DJ21-27	61.70	37.76	7.56	16.38
DJ21-32	60.66	35.62	8.08	16.96
DJ21-37	61.22	33.96	9.71	17.55
DJ21-43	61.60	33.30	9.94	18.36
DJ21-49	62.54	31.63	10.89	20.22
DJ21-57	61.52	27.99	12.47	21.06

increase of the rock thickness, and the transmitted energy increases accordingly. In dynamic loading combination behind the rock specimen with concrete cushion, the absorbed energy decreases with the increase of rock-accounted concrete. When the rock is 25 mm, the total absorption energy reached its lowest point; when the thickness of the rock is greater than the thickness of concrete, concrete and adjacent parts of rock joint cushion absorb the energy into a rising trend. Since incident energy = reflected energy + transmitted energy + absorbed energy, the variation trend of the reflected energy decreases with the absorbed energy and transmitted energy when incident energy is basically unchanged. On the whole, the reflected energy is the largest, and the absorbed energy and transmitted energy decrease successively. There is a significant difference between the three energies, as shown in Figure 9. The quadratic fitting polynomial is

$$\begin{cases} W_R = -5.7 \times 10^{-3}L^2 + 0.099L + 38.046 \left(R^2 = 0.9663\right), \\ W_D = 7.17 \times 10^{-3}L^2 - 0.362L + 21.478 \left(R^2 = 0.9532\right), \\ W_T = 7.30 \times 10^{-4}L^2 + 0.143L + 3.2932 \left(R^2 = 0.9851\right), \end{cases}$$
(5)

where W_R, W_D, and W_T represent reflected energy, absorbed energy, and transmitted energy.

3.6. Failure Mode Analysis of Specimens. Figure 10 shows the dynamic compression failure patterns of rock-concrete composite specimens with different thickness ratios.

As can be seen from Figure 10, under the same loading pressure, with the increase of the proportion of rock in the combination, the degree of breakage of the specimen
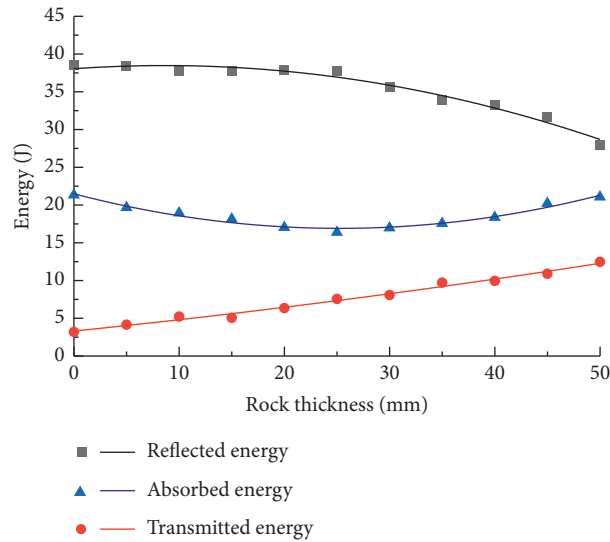
FIGURE 9: Curve of relation between rock thickness and reflected energy, absorbed energy, and transmitted energy.
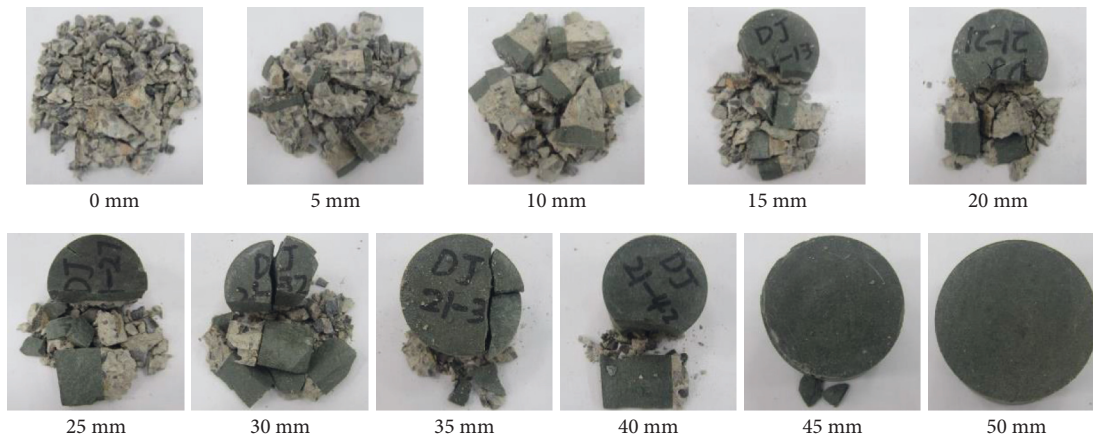

FIGURE 10: Dynamic compaction damages the morphology of rock-concrete combined bodies with different thickness ratios.

gradually decreases. When both the rock part and the concrete part are broken, the concrete part is in the majority and the particle size is smaller; this is because concrete acts as a buffer behind the rock when the specimen is impacted. Concrete absorbs more energy and has a weaker texture, resulting in more serious breakage. Some fragments fracture when the rock and concrete separate at the bonding surface because the rock-concrete interface is weak relative to the material on either side.

4. Conclusion

The SHPB impact compression test of ϕ 50 mm × 50 mm rock-concrete composite specimen with different thickness ratios was carried out under the same impact pressure, the mechanical properties of the composite and its changing rules were analyzed, the failure characteristics of the rock-concrete composite specimen with different thickness ratios under the same impact pressure were discussed, and the following conclusions were drawn:

(1) With the increase of the proportion of rock in the composite, the dynamic compressive strength and dynamic elastic modulus increase gradually, and the rock part is the main undertaker of the strength of the composite. The average strain rate decreases and the peak strain decreases, and the concrete part is the main undertaker of the deformation of the composite body.

(2) In dynamic loading combination behind the rock specimen with concrete cushion, absorption energy decreases with the increase of rock-accounted concrete. When the rock is 25 mm, the total absorption energy reached its lowest point; when the thickness of the rock is greater than the thickness of concrete, concrete and adjacent parts of rock joint cushion absorb the energy into a rising trend.

(3) Under the same air pressure, the degree of fragmentation of rock-concrete composite specimens with different thickness ratios decreases gradually with the increase of the proportion of rock. The

fragments are mainly concrete with a smaller particle size, which is correlated with the dynamic compressive strength. As the rock-concrete interface is a weak surface relative to the materials on both sides, part of the broken pieces are separated from the rock and concrete at the bonding surface.

Data Availability

The data used to support the findings of this study are available from the corresponding author upon request.

Conflicts of Interest

The authors declare that there are no conflicts of interest regarding the publication of this paper.

Acknowledgments

References

[1] H.-L. Qu, H. Luo, H. Hu, H. Y. Jia, and D. Zhang, "Dynamic response of anchored sheet pile wall under ground motion: analytical model with experimental validation," *Soil Dynamics and Earthquake Engineering*, vol. 115, pp. 896–906, 2018.

[2] H. Qu, Y. Deng, Y. Gao, X. Huang, and Z. Zhang, "Time history of seismic earth pressure response from gravity retaining wall based on energy dissipation," *Journal of Mountain Science*, vol. 19, no. 2, pp. 578–590, 2022.

[3] Q. Ping, H. P. Su, D. D. Ma, H. Zhang, and C. L. Zhang, "Experimental study on physical and dynamic mechanical properties of limestone after different high temperature treatments," *Rock and Soil Mechanics*, vol. 42, no. 4, pp. 932–942+953, 2021.

[4] Q. Ping, M. J. Wu, P. Yuan, and H. Zhang, "Experimental study on dynamic mechanical properties of high temperature sandstone under impact loads," *Chinese Journal of Rock Mechanics and Engineering*, vol. 38, no. 4, pp. 782–792, 2021.

[5] Q. Ping, C. L. Zhang, and H. J. Sun, "Experimental study on dynamic characteristics of sandstone after different high temperature cyclings," *Journal of Mining and Safety Engineering*, vol. 38, no. 5, pp. 1015–1024, 2021.

[6] J. P. Zuo, Y. Chen, and F. Cui, "Investigation on mechanical properties and rock burst tendency of different coal-rock combined bodies," *International Journal of Mining Science and Technology*, vol. 47, no. 1, pp. 81–87, 2018.

[7] X. Y. Liu, Y. C. Ye, Q. H. Wang, H. Zhang, Y. Z. Liu, and Y. Liu, "Mechanical properties of similar material specimens of composite rock masses with different strengths under uniaxial compression," *Rock and Soil Mechanics*, vol. 38, no. S2, pp. 183–190, 2017.

[8] P. X. Zhao, Y. C. He, and S. G. Li, "Coal thickness effect on mechanics and energy characteristics of coal-rock combination model," *Journal of Mining and Safety Engineering*, vol. 37, no. 5, pp. 1067–1076, 2020.

[9] Z. Zhang, J. Liu, L. Wang, and H. T. Yang, "Effects of combination mode on mechanical properties and failure characteristics of the coal-rock combinations," *Journal of China Coal Society*, vol. 37, no. 10, pp. 1677–1681, 2012.

[10] F. Q. Gong, H. Ye, and Y. Luo, "Rate effect on the burst tendency of coal-rock combined body under low loading rate range," *Journal of China Coal Society*, vol. 42, no. 11, pp. 2852–2860, 2017.

[11] S. Zeng, N. Zhang, B. Sun, and D. Yuan, "Mechanical performance of uni-body bi-material model for rock-concrete under dry and saturated states," *Bulletin of the Chinese Ceramic Society*, vol. 37, no. 7, pp. 2206–2209, 2018.

[12] J. Y. Teng, J. X. Tang, and J. B. Wang, "The evolution law of the damage of bedded composite rock and its fractal characteristics," *Chinese Journal of Rock Mechanics and Engineering*, vol. 37, no. S1, pp. 3263–3278, 2018.

[13] Z. H. Zhu, T. Feng, and F. Q. Gong, "Experimental research of mechanical properties on grading cycle loading-unloading behavior of coal-rock combination bodies at different stress levels," *Journal of Central South University*, vol. 47, no. 7, pp. 2469–2475, 2016.

[14] K. Yang, W. J. Liu, Y. K. Ma, R. J. Xu, and X. L. Chi, "Experimental study of impact failure characteristics of coal-rock combination bodies under true triaxial loading and single face unloading," *Rock and Soil Mechanics*, vol. 43, no. 1, pp. 15–27, 2022.

[15] H. Dong, "Mechanical response of coal rock mass with different proportions under true triaxial load," *Safety In Coal Mines*, vol. 52, no. 11, pp. 52–62, 2021.

[16] B. Chen and Q. Y. Ma, "Experiment and analysis on energy absorption characteristics and failure modes of concrete-frozen soil composite under impact loads," *Science Technology and Engineering*, vol. 19, no. 29, pp. 278–282, 2019.

[17] S. Wen, X. W. Zhao, and Y. L. Chang, "Dynamic compression damage energy dissipation analysis of composite rock samples based on SHPB," *Journal of Basic Science and Engineering*, vol. 29, no. 2, pp. 483–492, 2021.

[18] Y. Yang, R. S. Yang, and J. G. Wang, "Simulation material experiment on dynamic mechanical properties of jointed rock affected by joint thickness," *Journal of China University of Mining and Technology*, vol. 45, no. 2, pp. 211–216, 2016.

[19] R. S. Yang, M. Y. Wang, Y. Yang, and J. G. Wang, "Simulation material experiment on the dynamic mechanical properties of jointed rock affected by joint-filling material," *Journal of Vibration and Shock*, vol. 35, no. 12, pp. 125–131, 2016.

[20] R. S. Yang, W. Y. Li, S. Z. Fang, Y. Zhu, and Y. Li, "Experimental study on impact dynamic characteristics of layered composite rocks," *Chinese Journal of Rock Mechanics and Engineering*, vol. 38, no. 9, pp. 1747–1757, 2019.

[21] D. M. Guo, P. Y. Yan, and L. F. Fan, "A study on the stress wave characteristics and dynamic mechanical property of the sprayed concrete-surrounding rock combined body," *Journal of Vibration and Shock*, vol. 37, no. 24, pp. 85–91+136, 2018.

[22] D. M. Guo, P. Y. Yan, and Y. S. Zhang, "Experimental research on the sprayed concrete-surrounding rock combined body subjected to cyclic impact loading," *Journal of Vibration and Shock*, vol. 38, no. 10, pp. 105–111, 2019.

[23] D. M. Guo, P. Y. Yan, L. F. Fan, Y. Zhang, and X. Wang, "Experimental study on dynamic mechanical properties of sprayed concrete-surrounding rock combined body," *Journal of Beijing Institute of Technology (Social Sciences Edition)*, vol. 28, no. 2, pp. 278–285, 2019.

[24] M. Chen, H. Wang, and M. Qi, "Experimental study on dynamic compressive properties of composite layers of rock and steel fiber reinforced concrete," *Chinese Journal of Rock Mechanics and Engineering*, vol. 39, no. 6, pp. 1222–1230, 2020.

[25] M. Chen, X. W. Cui, X. Yan, H. Wang, and E. L. Wang, "Prediction model for compressive strength of rock-steel fiber reinforced concrete composite layer," *Rock and Soil Mechanics*, vol. 42, no. 3, pp. 638–646, 2021.

[26] L. G. Miao, Y. Y. Niu, and B. M. Shi, "Impact dynamic tests for rock-coal-rock combination under different strain rates," *Journal of Vibration and Shock*, vol. 38, no. 17, pp. 137–143, 2019.

[27] S. Chines, "Chinese society for rock mechanics and engineering," 2019, https://www.ttbz.org.cn/Home/Show/10253.

[28] Q. Ping, M. Wu, Q. Ma, P. Yuan, and H. Zhang, "Comparison and selection analysis of reasonable loading waveform in SHPB test," *Journal of Underground Space and Engineering*, vol. 13, no. 6, pp. 1499–1505, 2017.